crcB KO cells. These findings suggest that CrcB protein is important for reducing fluoride concentrations in cells, thus reducing its toxicity.

Another gene family commonly associated with fluoride riboswitches is a distinct subset of highly related *eriC* genes (hereafter called *eriC^F*) coding for ClC-type ion channel proteins. The prototypic *eriC* representatives exhibit specificity for chloride (fig. S13) (*17–19*). However, EriC^F protein homologs commonly associated with fluoride riboswitches carry a distinct set of amino acids in their putative channels compared with validated chloride-specific EriC proteins (fig. S14). This finding suggests that members of the EriC^F subgroup could be channels for fluoride anions. Anion flux assays conducted with the EriC^F protein from *P. syringae* reveal similar efficiency for chloride and fluoride transport (Fig. 3C), whereas a typical EriC protein from *E. coli* greatly favors chloride over fluoride (Fig. 3D).

We assessed the biological function of the EriC^F variant from *P. syringae* by expressing the protein in the *E. coli* strain lacking the CrcB protein. Consistent with fluoride transport activity, the *P. syringae eriC^F* gene rescues growth of the *E. coli crcB* KO strain to yield cells with restored resistance to high fluoride concentrations in both liquid and solid media (fig. S15). The functional equivalency of EriC^F and CrcB proteins is likewise suggested by their distributions among bacterial species (fig. S16). The genes for these putative fluoride transport proteins are rarely observed in the same species under the control of fluoride riboswitches, suggesting that their biochemical roles may be identical.

crcB genes associated with fluoride riboswitches are distributed broadly among bacteria and archaea (fig. S16). Riboswitches are associated with genes for CrcB proteins that vary greatly in amino acid sequence (fig. S17), suggesting that all CrcB proteins might have the same function in mitigating fluoride toxicity. If true, a surprisingly large number of organisms are predicted to contend with fluoride toxicity, including eukaryotic lineages such as fungi and plants. Moreover, the bacterium *Streptococcus mutans* (a causative agent of dental caries) encodes EriC^F proteins in the same genomic location where other *Streptococcus* species encode CrcB proteins (fig. S18). This arrangement again supports the hypothesis that the proteins are functionally equivalent and reveals the importance of fluoride toxicity resistance for *S. mutans*.

Though the vast majority of species encode at most 2 fluoride riboswitches, the bacterium *Methylobacterium extorquens* DM4 encodes at least 10 fluoride riboswitches in its genome. This organism, known for its ability to consume halogenated hydrocarbons as a food source (*20*), has been shown to survive on dichloromethane. The pertinent halogenase enzyme can catalyze the degradation of dibromomethane (*21*), suggesting that this organism also might degrade fluorinated hydrocarbons, which would generate fluoride anions and require a more robust fluoride sensor

and toxicity mitigation response system for rapid growth on fluorinated food sources.

Our findings resolve a long-standing mystery regarding why some species carry sensor and mitigation systems for toxic metals such as arsenic, cadmium, lead, and silver, whereas an analogous fluoride-specific system had been notably absent (*22*). The pervasive occurrence of these fluoride toxicity mitigation systems is consistent with the fact that fluorine is the 13th most abundant element in Earth's crust. Given their wide distributions, fluoride-specific riboswitches and commonly associated proteins such as CrcB may represent components of an ancient system by which cells have contended with toxic levels of this anion.

References and Notes
1. R. J. Lesher, G. R. Bender, R. E. Marquis, *Antimicrob. Agents Chemother.* **12**, 339 (1977).
2. M. Maltz, C. G. Emilson, *J. Dent. Res.* **61**, 786 (1982).
3. R. E. Marquis, S. A. Clock, M. Mota-Meira, *FEMS Microbiol. Rev.* **26**, 493 (2003).
4. R. S. Levine, *Br. Dent. J.* **140**, 9 (1976).
5. H. Koo, *Adv. Dent. Res.* **20**, 17 (2008).
6. I. R. Hamilton, *J. Dent. Res.* **69**, spec. no. 660, discussion 682 (1990).
7. C. Van Loveren, *Caries Res.* **35**, 65 (2001).
8. Z. Weinberg *et al.*, *Genome Biol.* **11**, R31 (2010).
9. Supporting text and materials and methods are available as supporting material on *Science* Online.
10. G. A. Soukup, R. R. Breaker, *RNA* **5**, 1308 (1999).
11. E. E. Regulski, R. R. Breaker, *Methods Mol. Biol.* **419**, 53 (2008).
12. J. T. Dobbins, H. A. Ljung, *J. Chem. Educ.* **12**, 586 (1935).
13. P. Auffinger, L. Bielecki, E. Westhof, *Structure* **12**, 379 (2004).
14. K. H. Hu *et al.*, *Genetics* **143**, 1521 (1996).
15. M. Rapp, E. Granseth, S. Seppälä, G. von Heijne, *Nat. Struct. Mol. Biol.* **13**, 112 (2006).
16. R. D. Finn *et al.*, *Nucleic Acids Res.* **38**, D211 (2010).
17. K. Matulef, M. Maduke, *Mol. Membr. Biol.* **24**, 342 (2007).
18. R. Dutzler, E. B. Campbell, M. Cadene, B. T. Chait, R. MacKinnon, *Nature* **415**, 287 (2002).
19. A. Accardi, C. Miller, *Nature* **427**, 803 (2004).
20. R. Gälli, T. Leisinger, *Conserv. Recy.* **8**, 91 (1985).
21. S. Vuilleumier, H. Sorribas, T. Leisinger, *Biochem. Biophys. Res. Commun.* **238**, 452 (1997).
22. S. Silver, *Gene* **179**, 9 (1996).

Erasure of a Spinal Memory Trace of Pain by a Brief, High-Dose Opioid Administration

Ruth Drdla-Schutting, Justus Benrath,* Gabriele Wunderbaldinger, Jürgen Sandkühler†

Painful stimuli activate nociceptive C fibers and induce synaptic long-term potentiation (LTP) at their spinal terminals. LTP at C-fiber synapses represents a cellular model for pain amplification (hyperalgesia) and for a memory trace of pain. μ-Opioid receptor agonists exert a powerful but reversible depression at C-fiber synapses that renders the continuous application of low opioid doses the gold standard in pain therapy. We discovered that brief application of a high opioid dose reversed various forms of activity-dependent LTP at C-fiber synapses. Depotentiation involved Ca^{2+}-dependent signaling and normalization of the phosphorylation state of α-amino-3-hydroxy-5-methyl-4-isoxazolepropionic acid receptors. This also reversed hyperalgesia in behaving animals. Opioids thus not only temporarily dampen pain but may also erase a spinal memory trace of pain.

μ-Opioid receptors (MORs) are expressed on spinal terminals of nociceptive C-fiber afferents and mediate the acute and quickly reversible presynaptic depression by opioids, mainly via inhibition of N- and P/Q-type voltage-gated calcium channels (*1*). In addition, brief activation of postsynaptic MORs triggers a rise in postsynaptic Ca^{2+} levels by increasing Ca^{2+} influx through *N*-methyl-D-aspartate (NMDA)–receptor channels (*2*) and by releasing Ca^{2+} from ryanodine-sensitive intracellular Ca^{2+} stores (*3*).

The acute synaptic depression and the prevention of synaptic plasticity by opioids have been studied extensively (*4–6*). In contrast, surprisingly little is known about the potential induction of Ca^{2+}-dependent synaptic plasticity by opioids.

Synaptic long-term potentiation (LTP) is a cellular model for learning and memory formation. The reversal of LTP, that is, synaptic depotentiation, is a potential mechanism of memory erasure (7). Depotentiation involves Ca^{2+}-dependent signaling (8) and may reverse LTP-associated changes in the phosphorylation state of α-amino-3-hydroxy-5-methyl-4-isoxazolepropionic acid receptors (AMPARs) (9). We tested the hypothesis that brief application of a MOR agonist reverses LTP at C-fiber synapses in superficial lumbar dorsal horn by Ca^{2+}-dependent signaling pathways, which normalize the phosphorylation state of AMPAR subunits.

In adult rats, conditioning low-frequency stimulation (LFS) of sciatic nerve fibers at C-fiber intensity induced LTP of spinal C fiber–evoked field potentials (10) (Fig. 1A). Brief intravenous infusion of a high dose of the ultrashort-acting MOR agonist remifentanil ($450~\mu g \cdot kg^{-1} \cdot hour^{-1}$) acutely depressed potentiated responses. Upon termination of the remifentanil infusion, C fiber–evoked field potentials did not return to the elevated predrug levels but were significantly depotentiated from $188 \pm 11\%$ to $128 \pm 14\%$ of control values before LFS ($n = 25$, $P < 0.001$, Fig. 1B). This is in contrast to the potentiation of C fiber–evoked field potentials upon wash-out of remifentanil in naïve animals (3, 11) and thus cannot be explained by an incomplete wash-out of the opioid. A second application of remifentanil given 1 hour later fully reversed LTP [depotentiation from $180 \pm 11\%$ (mean $\pm$ SEM) to $128 \pm 16\%$ of control after the first application, $P = 0.001$; and to $76 \pm 14\%$ after second application, $P < 0.001$; $n = 6$, Fig. 1C]. A lower dose of remifentanil ($225~\mu g \cdot kg^{-1} \cdot hour^{-1}$) was, however, ineffective ($196 \pm 22\%$ versus $194 \pm 12\%$ of control, $n = 5$, $P = 1$, Fig. 1D).

Our previous study revealed that abrupt but not tapered withdrawal from remifentanil induces LTP at naïve synapses (3). Here, the same tapering regimen had, in contrast, no effect on the efficacy of opioid-induced depotentiation (OID; depotentiation from $180 \pm 13\%$ to $123 \pm 10\%$, $n = 6$, $P = 0.002$; fig. S1A).

OID was unaffected by blockade of spinal γ-aminobutyric acid type A ($GABA_A$) receptors with picrotoxin (depotentiation from $216 \pm 19\%$ to $151 \pm 22\%$ of control, $n = 7$, $P = 0.001$; fig. S1B), indicating that an enhanced inhibition via $GABA_A$ receptors is not involved.

Acute depression and OID were fully blocked by intravenous application of the opioid receptor antagonist naloxone (fig. S1C) and by spinal application of the selective MOR antagonist D-Phe-

Cys-Tyr-D-Trp-Orn-Thr-Pen-Thr-NH$_2$ (CTOP, Fig. 2A), demonstrating that activation of spinal MORs is essential for both effects.

Withdrawal from opioids may trigger the release of glutamate and the activation of Ca^{2+}-permeable glutamate receptors of the NMDA subtype (12). The activation of group I metabotropic glutamate receptors (group I mGluRs) may lead to an additional rise in free cytosolic Ca^{2+} by Ca^{2+} release from intracellular stores. Blockade of Ca^{2+} entry through spinal NMDA receptors (Fig. 2B), blockade of group I mGluRs (Fig. 2C), or blockade of Ca^{2+} release from ryanodine-sensitive intracellular stores with dantrolene (Fig. 2D) all abolished OID but not the acute depression by the opioid.

LTP at the first synaptic relay in nociceptive pathways requires activation of Ca^{2+}/calmodulin-dependent protein kinase II and protein kinase C (PKC) (13, 14), which phosphorylate the GluR1 subunit of the AMPA receptor at Ser^{831} (15, 16). Interestingly, the time course of Ser^{831} phosphorylation in spinal dorsal horn parallels post-injury pain amplification (17) and is located to the superficial spinal dorsal horn (18), where C
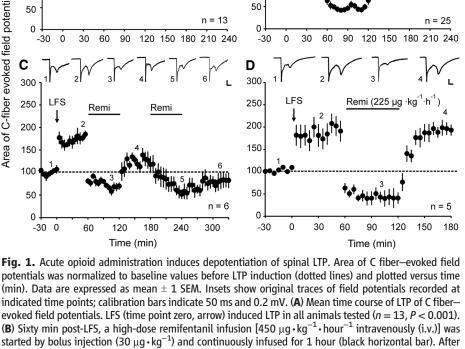
fibers terminate. Here, LFS-induced LTP was also associated with changes in the phosphorylation state of AMPARs, and we speculated that OID may reverse these changes. LFS caused enhanced phosphorylation of surface GluR1 subunits of AMPARs at Ser^{831} (S831-p; ratio of S831-p to total GluR1 protein levels was increased to $304 \pm 60\%$ of control, $n = 12$, $P = 0.006$). Remifentanil fully reversed this phosphorylation (ratio of S831-p to total GluR1 protein levels was $118 \pm 21\%$ of control, $n = 12$, $P = 0.41$ compared to control, $P = 0.007$ compared to LFS group; Fig. 3A). Dephosphorylation of spinal AMPARs at Ser^{831}, for example, by protein phosphatase 1 (PP1), reduces single-channel conductance and may thereby normalize synaptic strength (9). Accordingly, OID was completely prevented by blockade of PP1 (Fig. 2E).

LFS also induced a dephosphorylation of GluR2 subunits of AMPARs at Ser^{880} (S880-p) in the spinal dorsal horn (ratio of S880-p to total GluR2 protein levels was reduced to $67 \pm 10\%$ of control, $n = 12$, $P = 0.007$; Fig. 3B). After the opioid application, Ser^{880} was rephosphorylated (ratio of S880-p to total GluR2 protein levels

Fig. 1. Acute opioid administration induces depotentiation of spinal LTP. Area of C fiber–evoked field potentials was normalized to baseline values before LTP induction (dotted lines) and plotted versus time (min). Data are expressed as mean $\pm$ 1 SEM. Insets show original traces of field potentials recorded at indicated time points; calibration bars indicate 50 ms and 0.2 mV. (**A**) Mean time course of LTP of C fiber–evoked field potentials. LFS (time point zero, arrow) induced LTP in all animals tested ($n = 13$, $P < 0.001$). (**B**) Sixty min post-LFS, a high-dose remifentanil infusion [$450~\mu g \cdot kg^{-1} \cdot hour^{-1}$ intravenously (i.v.)] was started by bolus injection ($30~\mu g \cdot kg^{-1}$) and continuously infused for 1 hour (black horizontal bar). After wash-out of the drug, LTP was depotentiated ($n = 25$, $P < 0.001$). (**C**) A second infusion of high-dose remifentanil, which was started 60 min after the first one, abolished LTP after wash-out of the opioid ($n = 6$, $P < 0.001$). (**D**) Remifentanil infusion at a low dose ($225~\mu g \cdot kg^{-1} \cdot hour^{-1}$ i.v.) did not depotentiate LTP ($n = 5$, $P = 1$) after wash-out of the drug. In all graphs, statistical significance was determined by using one-way repeated measures analysis of variance (RM ANOVA).
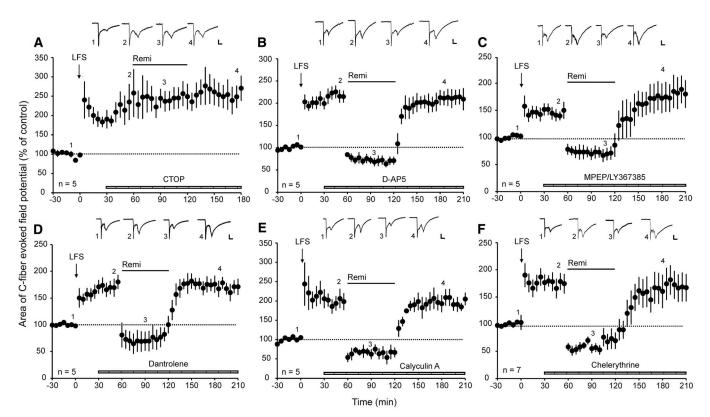
Department of Neurophysiology, Center for Brain Research, Medical University of Vienna, A-1090 Vienna, Austria.

*Present address: Centre of Pain Therapy, Clinic of Anaesthesia and Intensive Care, University Medical Centre Mannheim, Medical Faculty Heidelberg University, D-68167 Mannheim, Germany.
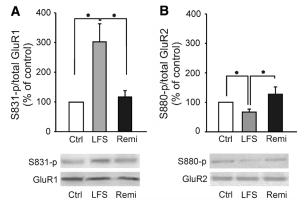
†To whom correspondence should be addressed. E-mail: juergen.sandkuehler@meduniwien.ac.at

Fig. 2. Signaling pathways involved in opioid-induced depotentiation. LTP induction and remifentanil application as in Fig. 1. Different blockers were applied directly onto the spinal cord at the recording segment (dashed horizontal bars). Insets show original traces of field potentials recorded at indicated time points; calibration bars, 50 ms and 0.2 mV. (**A**) Spinal superfusion with the MOR antagonist CTOP (10 μM) abolished acute depression and depotentiation in all animals tested ($n = 5$, $P = 1$). (**B** to **F**), OID was prevented by topical application of the NMDA receptor antagonist D-AP5 (100 μM, $n = 5$, $P = 1$), the mGluR antagonists MPEP (100 μM) and LY367385 (300 μM, $n = 5$, $P = 0.6$), the ryanodine receptor blocker dantrolene (500 μM, $n = 5$, $P = 1$), the PP1 inhibitor calyculin A (300 nM, $n = 5$, $P = 1$), or the PKC blocker chelerythrine (800 μM, $n = 7$, $P = 1$). In all experiments, statistical significance was determined by using a one-way RM ANOVA.

Fig. 3. Quantitative analysis of phosphorylation of surface AMPAR subunits after LFS and opioid treatment. Bar graphs summarize the ratio of phospho-GluR1-Ser[831] (S831-p) with total GluR1 (A) and ratio of phospho-GluR2-Ser[880] (S880-p) with total GluR2 (B). Data are expressed as mean + 1 SEM. Tissue samples were taken from naïve animals (Ctrl, $n = 12$), from animals 180 min post-LFS (LFS, $n = 12$), or from animals 180 min post-LFS with an additional 60-min remifentanil infusion (Remi, $n = 12$). Representative, corresponding Western blots are shown at the bottom.

*$P < 0.05$. (**A**) LFS induced phosphorylation of AMPAR GluR1 subunits at Ser[831], which was reversed by opioid treatment. (**B**) LFS dephosphorylated AMPAR GluR2 subunits at Ser[880], whereas remifentanil induced rephosphorylation at this site.

was $127 \pm 23\%$ of control, $n = 12$, $P = 0.028$; Fig. 3B). PKC phosphorylates GluR2 subunit at Ser[880]. This reduces glutamatergic synaptic transmission by promoting receptor endocytosis (19). Consistently, blockade of PKC fully prevented OID without affecting acute depression (Fig. 2F). We found no evidence for significant changes in

the phosphorylation state of GluR1 subunit of the AMPAR at Ser[845] after LFS (ratio of S845-p to total GluR1 protein levels was $160 \pm 38\%$ of control, $n = 12$, $P = 0.142$) or after opioid application ($93 \pm 17\%$ of control, $n = 12$, $P = 0.706$). The above described changes in the phosphorylation state of the AMPAR after LFS may enhance
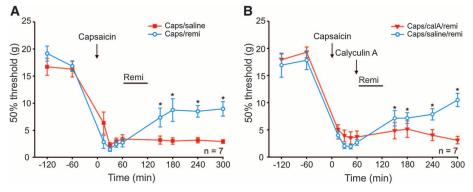
glutamatergic synaptic transmission (9), and their reversal may thus lead to OID.

The induction phase of spinal LTP, which lasts for 1 to 3 hours, involves posttranslational modifications, including changes in the phosphorylation state of synaptic proteins. The maintenance phase of LTP [>3 hours in spinal cord (20) and brain (21)] may in addition also involve de novo protein synthesis. We thus asked whether LTP in the maintenance phase can also be depotentiated by opioids. When remifentanil was given 4 hours after LTP induction, OID was as effective (depotentiation from $193 \pm 22\%$ to $131 \pm 14\%$, $n = 10$, $P = 0.028$; fig. S2, A and B) as when given after 1 hour. The reversal of late-phase LTP by remifentanil was, in contrast to that of early-phase LTP, not blocked by the PP1 inhibitor calyculin A ($220 \pm 22\%$ versus $156 \pm 20\%$, $n = 10$, $P = 0.024$; fig. S2C).

The persistently active protein kinase Mζ (PKMζ) is required in the spinal cord for maintaining tactile allodynia after intraplantar injection of interleukin-6 (22). We thus asked whether PKMζ in spinal cord also plays a role for the maintenance phase of LTP (22, 23) after LFS. PKMζ inhibitor ZIP had, however, no obvious

Fig. 4. Capsaicin-induced mechanical hyperalgesia is reduced after opioid administration. Capsaicin injection (time point zero, arrow) significantly reduced mechanical withdrawal thresholds in the ipsilateral paw of awake, drug-free rats. (**A**) One group of animals received a 1-hour high-dose remifentanil infusion (horizontal bar) 60 min after capsaicin injection (blue circles, n = 7). A control group was treated with an intravenous saline infusion (red squares, n = 7). After wash-out of the opioid, mechanical thresholds were elevated significantly compared with thresholds before opioid treatment at 150 min ($P = 0.05$), 180 min ($P = 0.003$), 240 min ($P = 0.004$), and 300 min ($P = 0.002$), indicating partial reversal of hyperalgesia. (**B**) Opioid-induced reduction of mechanical hyperalgesia is blocked by the PP1 inhibitor calyculin A. After capsaicin injection, calyculin A (300 nM, 10 μl) was injected intrathecally 10 min before a 1-hour high-dose remifentanil infusion (red triangles, n = 7). Intrathecal injections of saline served as control (blue circles, n = 7). After wash-out of the opioid, mechanical thresholds were elevated significantly compared with thresholds before opioid treatment in the control group at 150 min ($P = 0.021$), 180 min ($P = 0.019$), 240 min ($P = 0.003$), and 300 min ($P < 0.001$). No effect of the opioid treatment on mechanical thresholds could be observed in the calyculin A–treated group ($P = 0.523$). One-way RM ANOVA or RM ANOVA on ranks was used for statistical comparisons.

effect on the maintenance of LFS-induced LTP within the observation period of 6 hours (fig. S2D).

Depending on the type of conditioning stimulation, distinct forms of LTP are induced at C-fiber synapses, which affect different groups of postsynaptic neurons (13, 24) and involve signaling pathways that overlap only partially (13, 24, 25). We therefore tested whether OID can also be achieved for other forms of established spinal LTP. We induced LTP by conditioning high-frequency stimulation (HFS, 100 Hz; fig. S3A) of sciatic nerve fibers or by subcutaneous capsaicin injections (fig. S3C). The latter selectively activates nociceptive nerve fibers, which express the transient receptor potential channel subfamily V member 1 (TRPV1). Remifentanil also fully reversed these forms of LTP (after HFS, depotentiation was from $158 \pm 8\%$ to $99 \pm 9\%$, $n = 12$, $P < 0.001$; after capsaicin, depotentiation was from $170 \pm 16\%$ to $100 \pm 13\%$, $n = 5$, $P < 0.001$; fig. S3, B and D), demonstrating that OID applies to various forms of activity-dependent LTP at C-fiber synapses.

LTP is a synaptic model for some forms of hyperalgesia (26). We therefore asked whether OID has any relevance for behaving animals. Subcutaneous injections of capsaicin quickly led to mechanical hyperalgesia at the injected hindpaw (Fig. 4). The same dosage regimen of remifentanil that caused OID significantly attenuated capsaicin-induced hyperalgesia (Fig. 4A). Not surprisingly, the behavioral hyperalgesia was reversed only partially by the opioid treatment because additional peripheral and central mechanisms contribute to capsaicin-induced hyperalgesia (27, 28). PP1 inhibitor calyculin A fully blocked the attenuation of hyperalgesia by remifentanil (Fig. 4B), suggesting that depotentiation at nociceptive C fibers may erase a memory trace of pain. LTP is expressed in ascending nociceptive pathways, which are relevant for the aversive components of pain. It will thus be interesting to explore whether opioids may also reverse the tonic-aversive state of pain (29).

Taken together, the present and our previous data (3) demonstrate that activation of spinal MORs triggers distinct, bidirectional, and state-dependent synaptic plasticity in naïve versus potentiated C-fiber synapses. Remifentanil activates Ca^{2+}-dependent signaling pathways, leading to activation of PP1 and PKC. At potentiated synapses, this normalizes the phosphorylation state of GluR1 at Ser^{831} and that of GluR2 at Ser^{880}

and thereby depotentiates synaptic strength in C fibers. The presently identified reversal of synaptic LTP in nociceptive pathways provides a rationale for novel therapeutic strategies to cure rather than to temporarily dampen some forms of pain with opioids.

References and Notes

1. B. Heinke, E. Gingl, J. Sandkühler, *J. Neurosci.* **31**, 1313 (2011).
2. L. Chen, L.-Y. M. Huang, *Neuron* **7**, 319 (1991).
3. R. Drdla, M. Gassner, E. Gingl, J. Sandkühler, *Science* **325**, 207 (2009).
4. G. W. Terman, C. L. Eastman, C. Chavkin, *J. Neurophysiol.* **85**, 485 (2001).
5. F. S. Nugent, E. C. Penick, J. A. Kauer, *Nature* **446**, 1086 (2007).
6. M. H. Ossipov, G. O. Dussor, F. Porreca, *J. Clin. Investig.* **120**, 3779 (2010).
7. M. Zhuo et al., *Proc. Natl. Acad. Sci. U.S.A.* **96**, 4650 (1999).
8. C.-C. Huang, Y.-C. Liang, K.-S. Hsu, *J. Biol. Chem.* **276**, 48108 (2001).
9. H.-K. Lee, M. Barbarosie, K. Kameyama, M. F. Bear, R. L. Huganir, *Nature* **405**, 955 (2000).
10. Materials and methods are available as supporting online material at *Science* Online.
11. C. Heinl, R. Drdla-Schutting, D. N. Xanthos, J. Sandkühler, *J. Neurosci.* **31**, 16748 (2011).
12. K. H. Jhamandas, M. Marsala, T. Ibuki, T. L. Yaksh, *J. Neurosci.* **16**, 2758 (1996).
13. H. Ikeda et al., *Science* **312**, 1659 (2006).
14. H.-W. Yang et al., *J. Neurophysiol.* **91**, 1122 (2004).
15. A. Barria, D. Muller, V. Derkach, L. C. Griffith, T. R. Soderling, *Science* **276**, 2042 (1997).
16. K. W. Roche, R. J. O'Brien, A. L. Mammen, J. Bernhardt, R. L. Huganir, *Neuron* **16**, 1179 (1996).
17. Y. Wang et al., *Neurochem. Res.* **36**, 170 (2011).
18. L. Fang, J. Wu, X. Zhang, Q. Lin, W. D. Willis, *Neuroscience* **122**, 237 (2003).
19. H. J. Chung, J. Xia, R. H. Scannevin, X. Zhang, R. L. Huganir, *J. Neurosci.* **20**, 7258 (2000).
20. N.-W. Hu et al., *J. Neurophysiol.* **89**, 2354 (2003).
21. P. V. Nguyen, T. Abel, E. R. Kandel, *Science* **265**, 1104 (1994).
22. M. N. Asiedu et al., *J. Neurosci.* **31**, 6646 (2011).
23. T. C. Sacktor, *Nat. Rev. Neurosci.* **12**, 9 (2011).
24. H. Ikeda, B. Heinke, R. Ruscheweyh, J. Sandkühler, *Science* **299**, 1237 (2003).
25. R. Drdla, J. Sandkühler, *Mol. Pain* **4**, 18 (2008).
26. J. Sandkühler, *Physiol. Rev.* **89**, 707 (2009).
27. W. D. Willis Jr., *Exp. Brain Res.* **196**, 5 (2009).
28. D. Julius, A. I. Basbaum, *Nature* **413**, 203 (2001).
29. T. King et al., *Nat. Neurosci.* **12**, 1364 (2009).